Colloid Polym Sci (2008) 286:639–646
DOI 10.1007/s00396-007-1804-8

ORIGINAL CONTRIBUTION

# Microstructure of *N*,*N*′-bis(cetyldimethyl)-α,ω-propanediammonium dibromide micelle and its dynamics in solution studied by $^1$H NMR

**Xiao-Yan Yang · Hong Chen · Gong-Zhen Cheng ·**
**Shi-Zhen Mao · Mai-Li Liu · Ping-Ya Luo · You-Ru Du**

Received: 11 April 2007 / Revised: 10 November 2007 / Accepted: 13 November 2007 / Published online: 11 December 2007

**Abstract** The characteristics of *N*,*N*′-bis(cetyldimethyl)-α,ω-alkane (propane and butane) diammonium dibromide (16-3-16 and 16-4-16) aqueous solutions were studied by one- and two-dimensional $^1$H nuclear magnetic resonance (NMR). The measurements of self-diffusion coefficient and inter-proton distance at 318 K suggest that 16-3-16 spherical micelles are formed in the dilute solution at a concentration of 0.26 mmol/l and the polar head groups of the surfactant are in a saw-toothed form staying at the surface of the micelle to overcome the strong electrostatic repulsion force. Relaxation measurements obviously show that the spacer chain is rigid in the surface layer of the hydrophobic micellar core, and the side alkyl chains of 16-3-16 are packed more tightly than those of 16-4-16 in the micellar core. The line-shape analysis of the methyl protons at the end of the side alkyl chain of 16-3-16 and 16-4-16 suggests that two possible momentary morphologies of their side alkyl chains are situated in the micelle, respectively.

**Keywords** Gemini surfactant · *N*,*N*′-bis(cetyldimethyl)-α,ω-alkane diammonium dibromide (16-3-16 · 16-4-16) · Micelle · NMR

## Introduction

A new class of surfactant is presently attracting considerable interest in both the academic and industrial circles. These surfactants are made up of two or more amphiphilic moieties connected at the level of the head groups or very close to the head groups by a spacer group, which are referred to as gemini surfactants [1–3]. A series of alkanediyl-α,ω-bis (dimethylalky1ammonium bromide) surfactants, referred to as dimeric m-*s*-m surfactants (where m and *s* are the carbon numbers of the side alkyl backbone chains and of the spacer backbone chain, respectively), have been focused and investigated by various methods [4–21]. The physicochemical properties of *N*,*N*′-bis(cetyldimethyl)-α,ω-alkanediammonium dibromide (16-*s*-16) systems, both pure and mixed [3, 5, 7–13], have been studied extensively and provided much information on macroscopic and microscopic characteristics of gemini surfactant in aqueous solutions. In recent years, ever more types of gemini surfactants with different spacer chains have been reported to get deep information about the spacer effects [12–21]. However, less attention was paid on the properties of micelle in the relatively dilute 16-*s*-16 solutions [3, 22], which are slightly above the critical micelle concentration (CMC). The ladder model suggests that for a new-born micelle, having a minimum aggregation number indicates that the minute micelle may be spherical at

---

X.-Y. Yang · S.-Z. Mao (✉) · M.-L. Liu (✉) · Y.-R. Du
State Key Laboratory of Magnetic Resonance and Atomic and Molecular Physics, Wuhan Centre for Magnetic Resonance, Wuhan Institute of Physics and Mathematics,
Chinese Academy of Science,
Wuhan 430071, China
e-mail: maosz@wipm.ac.cn
e-mail: ml.liu@wipm.ac.cn

H. Chen · P.-Y. Luo
State Key Laboratory of Oil and Gas Reservoir Geology and Exploitation Engineering, Southwest Petroleum Institute,
Nanchong 637001, China

G.-Z. Cheng
College of Chemistry and Molecular Sciences, Wuhan University,
Wuhan 430072, China

X.-Y. Yang
School of Chemistry and Environmental Engineering, Changsha University of Science and Technology,
Changsha 410076, China

the CMC in aqueous solutions, and both micellar growth and shape variation occur with an increase in surfactant concentration [23]. Nuclear magnetic resonance (NMR) spectroscopy is a versatile technique for the study of surfactants [24]. To understand the micellization process and properties of the shape of micelles, we have studied the behavior of 14-2-14, 14-3-14, 14-4-14 and 16-4-16 in dilute aqueous solution by $^1$H NMR at 298 and 313 K in detail recently, respectively [25, 26]. The dynamics of these gemini surfactants and the relative arrangement of the side alkyl chains in the micelle show much difference from those of the conventional cationic surfactants. In this work, we intended to acquire the information about the relative arrangement of 16-3-16 molecules in the micelle and the microstructure of the compact surface layer of the micellar core, which is important for understanding the characteristic of micelles.

## Experimental

16-4-16 and 16-3-16 were synthesized by the Southwest Petroleum Institute. Cetyl-trimethyl ammonium bromide (CTAB) is an analytical-grade reagent produced by Jining Institute of Chemical Engineering of China. $D_2O$, 99.8% deuterated, is the product of the Wuhan Bopu Corporation of Chinese Academy of Sciences. They were used as received, without any further purification. $^1$H NMR experiments validate their quality of certainty. The CMCs of CTAB, 16-4-16, and 16-3-16 are 9.0 [27], 0.027, and 0.026 mmol/l [3] at 298 K, respectively. The concentrations of CTAB, 16-4-16, and 16-3-16 solutions are 45, 0.27, and 0.26 mmol/l, respectively. These solutions have been kept at ambient temperature for more than 2 weeks to ensure that equilibrium has been attained.

The Krafft point ($K_p$) of 16-4-16 and 16-3-16 are 310.5 and 316 K, respectively [5]. Consequently, NMR experiments for the 16-4-16 and 16-3-16 solutions were carried out at temperatures slightly above their $K_p$ temperatures, 313 and 318 K, respectively. NMR measurements are performed using a UNITY INOVA-500 spectrometer with a proton frequency of 500.123MHz. $D_2O$ was used as solvent instead of water to provide lock signal for NMR machine and to weaken the water signal, and the residual water signal was suppressed by presaturation. The standard pulse sequences provided by the Varian Corporation were used for the relative experiments. NMR tubes (5 mm) were used, and the samples were equilibrated in the probe for more than 30 min before the self-diffusion coefficient measurement. Convection within the sample is a serious problem affecting diffusion measurement, in particular at elevated temperature. To suppress effects of convection during the diffusion interval of the diffusion-pulse sequence at elevated temperatures and compensate eddy-current effects, Double-Stimulated-Echo experiment with bipolar gradient, provided by Jerschow A. and Muller N. [28], has been used previously in diffusion experiments. The self-diffusion coefficient is obtained by fitting the Stejskal-Tenner relation [29] to the signal intensities. The chemical shifts were estimated from the 3-(trimethylsilyl)propionate (TSP) external standard signal. Two-dimensional (2D) Nuclear Overhauser Enhancement Spectroscopy (NOESY) experiments [30] were performed for 16-4-16 and 16-3-16 solutions at experimental concentrations at 313 and 318 K, respectively.

## Results and discussions

### Results

The structures and proton numberings of CTAB, 16-4-16, and 16-3-16 are shown in Scheme 1. The corresponding $^1$H NMR one-dimensional (1D) spectra at the micellar states are shown in Fig. 1. Direct evidence about the space relationship among the surfactant molecules will help to confirm the arrangement of the molecules in the micelle. This can be achieved by the 2D NOESY experiment. To examine the evolution of cross-peaks in the 2D NOESY experiments of the 0.26 mmol/l 16-3-16 aqueous solutions, different mixing times of 50, 100, and 160 ms have been used. The intensity of the cross-peaks is increasing up to 160 ms as shown in Fig. 2. So it is safe to choose the mixing time of 100 ms to estimate the inter-proton distances to ensure that the intensities of the cross-peaks are not destroyed by spin diffusion. The contour plot of the 2D NOESY experiment with a mixing time of 100 ms is shown in Fig. 3. One can extract valuable information about inter-proton distances from the intensities of the cross-peaks with the aid of one known distance in the molecule. The following formula was used with the aid of the known distance 2–3 in the molecule and the corresponding cross-peak signal intensity:

$$\sqrt[6]{\frac{I_{23}}{I_{mn}}}=\frac{r_{mn}}{r_{23}}$$

where $I_{23}$ and $I_{\mathrm{mn}}$ are the intensities of the cross-peaks between 2 and 3 and between the two protons of interest, respectively, and $r_{23}$ and $r_{\mathrm{mn}}$ are the corresponding inter-proton distances. The inter-proton distances of 16-3-16 and 16-4-16 in the micellar state derived from the cross-peak intensities by the above formula and calculated by HyperChem on the basis of a single molecular state are shown in Table 1. The chemical shifts of methylene protons of $(CH_2)_{12}$, 4, are very close; they overlap seriously, so the

**Scheme 1** Structures and proton numberings of CTAB, 16-4-16, and 16-3-16

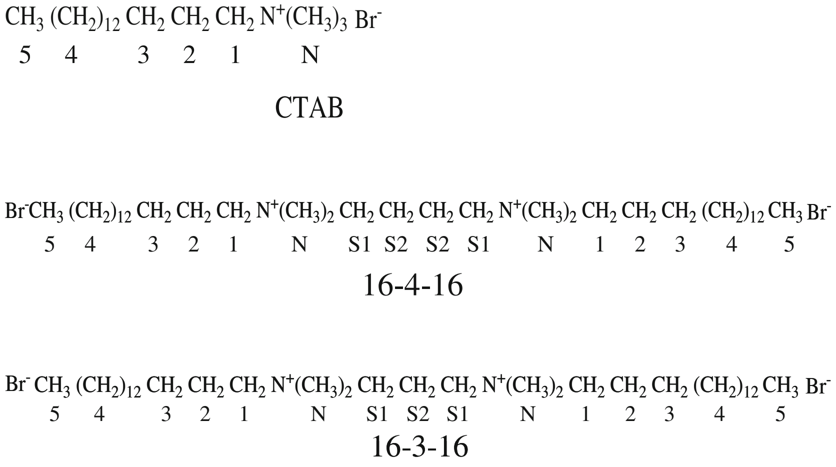

$CH_3\,(CH_2)_{12}\,CH_2\,CH_2\,CH_2\,N^+(CH_3)_3\,Br^-$

$Br^-CH_3\,(CH_2)_{12}\,CH_2\,CH_2\,CH_2\,N^+(CH_3)_2\,CH_2\,CH_2\,CH_2\,CH_2\,N^+(CH_3)_2\,CH_2\,CH_2\,CH_2\,(CH_2)_{12}\,CH_3\,Br^-$

$Br^-\,CH_3\,(CH_2)_{12}\,CH_2\,CH_2\,CH_2\,N^+(CH_3)_2\,CH_2\,CH_2\,CH_2\,N^+(CH_3)_2\,CH_2\,CH_2\,CH_2\,(CH_2)_{12}\,CH_3\,Br^-$

intensities of the cross-peaks of 4 with other protons are due to contributions from the portion of the 24 methylene segments and are not suitable to estimate the inter-proton distances. The same is for the intensities of the cross-peaks of S1(1) with other protons.

Self-diffusion coefficients of 16-3-16 and 16-4-16 solutions at a concentration of ten times their CMCs at 318 and 313 K, respectively (Table 2), suggest that 16-3-16 molecules are more densely packed in the micelle than 16-4-16 molecules are.

It is obvious in Fig. 1 that the chemical shifts of each of the corresponding proton peaks are in the order of 16-3-16 > 16-4-16 > CTAB. It is interesting to note that for 16-3-16, S1 overlaps with 1. To understand this phenomenon, 1D spectra of 14-3-14 and 14-4-14 were also traced for comparison. Their chemical shifts at different concentrations at 298 K are shown in Table 3. It is also worth to notice from Fig. 1 that the peaks of the methyl protons at the end of the side alkyl chain of 16-4-16 and 16-3-16 are two overlapped triplets, respectively, which differ from that of CTAB. These two bands were each deconvolved into two triplets of various areas, which are shown in Fig. 4, and the areas of the sub-peaks were monitored in the single-pulse experiment and shown in Table 4. In the same way, the areas of the sub-peaks were monitored for the spin-lattice relaxation ($T_1$) and the spin-spin relaxation ($T_2$) experiments, from which the $T_1$ and $T_2$ values were determined, also shown in Table 4.

The $T_2$ and $T_1$ values of 16-3-16 solution are compared with those of the CTAB solution at 298 K and 16-4-16 solution at 313 K, respectively, as shown in Fig. 5a and b. It

**Fig. 1** $^1$H NMR spectra for **a** CTAB solution of 45.0 mmol/l, **b** 16-4-16 solution of 0.27 mmol/l, and **c** 16-3-16 solution of 0.26 mmol/l at 298, 313, and 318 K, respectively

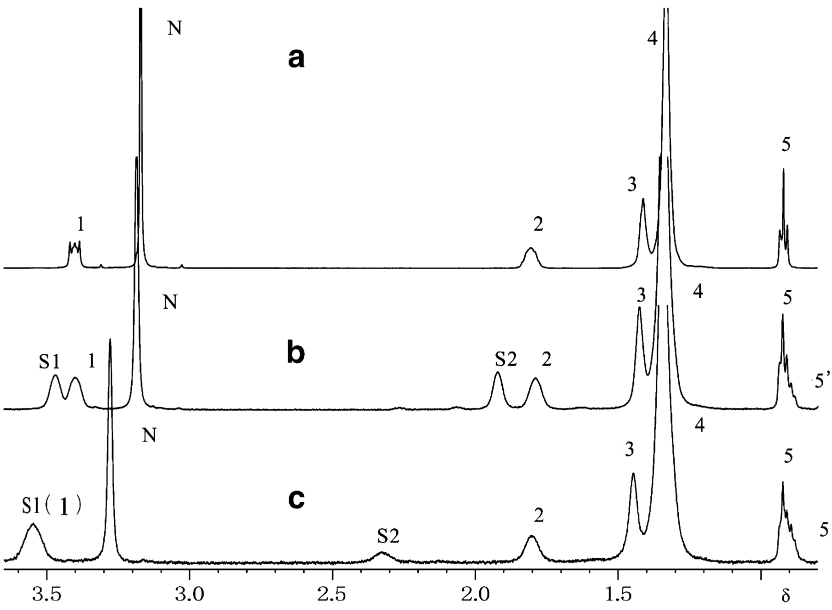

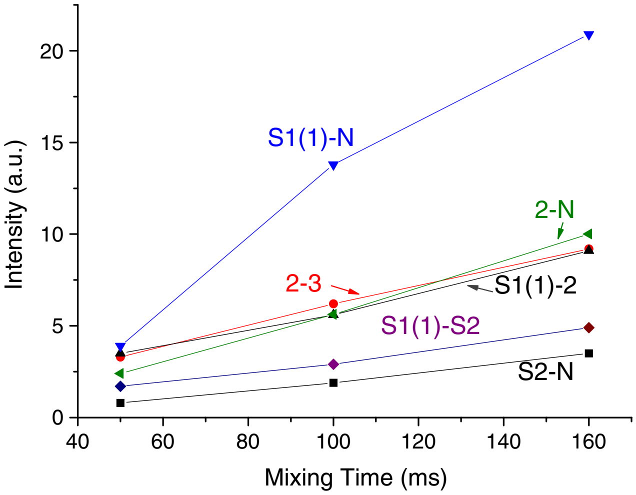

**Fig. 2** Evolution of the intensities of the cross-peaks of random proton pairs in the 2D NOESY spectra of 16-3-16 solution of 0.26 mmol/l as a function of the mixing time

is obvious that the spacer has significant effect on the motion of chains in the micelles. The shorter the spacer, the more seriously is the motion of protons on the alkyl side chain restricted. The decay behaviors of N and 3 of 16-3-16 are compared with those of 16-4-16, respectively, as shown in Table 5.

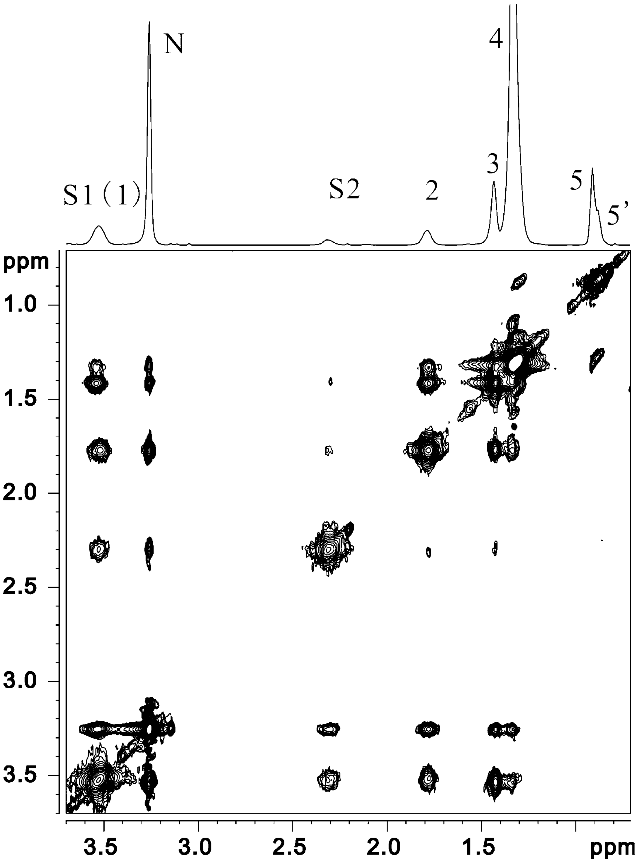

**Fig. 3** Contour plot of 2D NOESY spectrum of 16-3-16 solution of 0.26 mmol/l at 318 K with a mixing time of 100 ms

**Table 1** Inter-proton distances (Å) of 16-4-16 solution of 0.27 mmol/l at 313 K and 16-3-16 solution of 0.26 mmol/l at 318 K, respectively, calculated from the cross-peak intensities of the 2D NOESY spectra at a reliable mixing time and those of 16-3-16 calculated by HyperChem

| Proton pairs | $r_{16\text{-}3\text{-}16}$ (Å) | $r_{16\text{-}4\text{-}16}$ (Å) | $r_{\mathrm{HYP}}$ (Å) |
|---|---|---|---|
| 2–3 | 2.8 | 2.8 | 2.8 |
| 3–N | 4.0 | 4.1 | 5.1 |
| 2–N | 3.4 | 3.2 | 3.4 |
| S2–N | 4.1 | 3.4 | 4.0 |
| S2–3 | 4.7 | 4.0 | 5.0 |
| S2–2 | 4.4 | 3.8 | 4.8 |

The inter-proton distances were calculated by assuming the distance between 2 and 3 to be 2.8 Å, taken from the value calculated by HyperChem, and $r_{\mathrm{HYP}}$ represents the inter-proton distance calculated by HyperChem on the basis of a single molecular state.

## Discussions

### *Microstructure of 16-3-16 micelles*

We can choose the proton distance, calculated by HyperChem on the basis of a single 16-3-16 molecular state, as a relative standard to compare the configuration of the two surfactants situating in their micelles. Following Table 1, it is obvious that all of the inter-proton distances except that between N and 3 of 16-3-16 are almost the same within 10% error in the micelles, as compared with those calculated by HyperChem on the basis of a single 16-3-16 molecular state. Meanwhile, the inter-proton distances of S2-N, S2-2, and S2-3 proton pairs of 16-3-16 are about 0.7 Å larger than those of 16-4-16. All these suggest that the arrangement of 16-3-16 molecules is similar to that of 16-4-16 in the micellar states [25], except that S2 protons of 16-3-16 are extended outwards to the water medium than that of 16-4-16. The inter-proton distance of between N and 3 of 16-3-16 is shorter than those calculated by HyperChem and is the same as those of 16-4-16 [25]. It also implies that the head groups of 16-3-16 are in a saw-toothed form staying at the surface of the micelle. Following all of these, it can provide a picture of the molecule arrangement in the 16-3-16 micelle. The spacer extends toward the water medium with the polar heads arranged in a saw-toothed form to overcome the electrostatic repulsion force and the side alkyl chains of 16-3-16 molecules lying side by side.

**Table 2** The self-diffusion coefficient ($\times 10^{-11}$ m$^2$/s) of 16-4-16 and 16-3-16 solutions at a concentration of ten times their CMCs at 313 and 318 K, respectively

| | Solvent | Solute |
|---|---|---|
| 313 K (16-4-16) | 324 | 7.3 |
| 318 K (16-3-16) | 392 | 6.3 |

**Table 3** The chemical shifts of 14-3-14 and 14-4-14 protons at different concentrations at 298 K

| | $\Delta\delta_{0.5\ \mathrm{CMC}}$ ($\delta^{14\text{-}3\text{-}14}$–$\delta^{14\text{-}4\text{-}14}$) | 14-3-14 | | | 14-4-14 | | |
|---|---|---|---|---|---|---|---|
| | | $\delta_{0.5\mathrm{CMC}}$ | $\delta_{10\mathrm{CMC}}$ | $\Delta\delta$ | $\delta_{0.5\mathrm{CMC}}$ | $\Delta_{10\mathrm{CMC}}$ | $\Delta\delta$ |
| S1 | 0 | 3.39 | 3.56 | 0.17 | 3.39 | 3.48 | 0.09 |
| 1 | 0.07 | | | | 3.32 | 3.42 | 0.10 |
| N | 0.06 | 3.16 | 3.28 | 0.12 | 3.10 | 3.19 | 0.09 |
| S2 | 0.40 | 2.26 | 2.32 | 0.06 | 1.86 | 1.92 | 0.06 |
| 2 | 0.01 | 1.78 | 1.81 | 0.03 | 1.77 | 1.80 | 0.03 |
| 3 | 0.01 | 1.40 | 1.45 | 0.05 | 1.39 | 1.43 | 0.04 |
| 4 | 0 | 1.31 | 1.34 | 0.03 | 1.31 | 1.34 | 0.03 |
| 5 | 0 | 0.89 | 0.92 | 0.03 | 0.89 | 0.92 | 0.03 |

All of the proton numbers of proton groups of 14-*s*-14 except 4, which stand for methylene protons of $(CH_2)_{10}$, correspond to those of 16-*s*-16.

### *Hydrocarbon chain packing in the micelle*

The self-diffusion coefficient measurements of the 16-4-16 and 16-3-16 were determined by the Fourier Transform Pulsed-Gradient Spin-Echo NMR technique on the basis of their separate peaks at 313 and 318 K, respectively. The apparent self-diffusion coefficient derived from peak areas with the experimental error of less than 10% are shown in Table 2. At a concentration of ten times its CMC, the self-diffusion coefficient of 16-3-16 is about 16% lower than that of 16-4-16 solution at a concentration which is also ten times its CMC. Meanwhile, the self-diffusion coefficient of water molecules (HOD) of 16-3-16 solution is higher than that of 16-4-16 markedly, which are also shown in Table 2. According to the Einstein–Stokes equation, the self-diffusion coefficient of a particle is proportional to the absolute temperature. So the self-diffusion coefficient of 16-3-16 measured at 318 K should be higher than that of 16-4-16 at 313 K. Because both surfactants have the same alkyl side chains, the radii of the particles and their diffusion coefficients would not deviate very much. However, the result is converse. This phenomenon seems to originate from the difference in density of the particle, i.e., the micelle. The hydrodynamic radius of a micelle depends mainly on the length of the hydrophobic alkyl chain of the surfactant. Since 16-3-16 has the same alkyl chain as that of 16-4-16, their hydrodynamic radii of the micelles will not deviate very much. A lower value of the self-diffusion coefficient of 16-3-16 suggests that the density of the micelle is greater, which means that there are more alkyl chains (molecules of surfactant) in the micellar core for 16-3-16 than for 16-4-16 and, consequently, the larger the aggregation number. This can be understood by the effect of the length of the spacer. The shorter the spacer, the smaller the area of the polar head that occupies the surface of the micellar core, consequently, the more surfactant

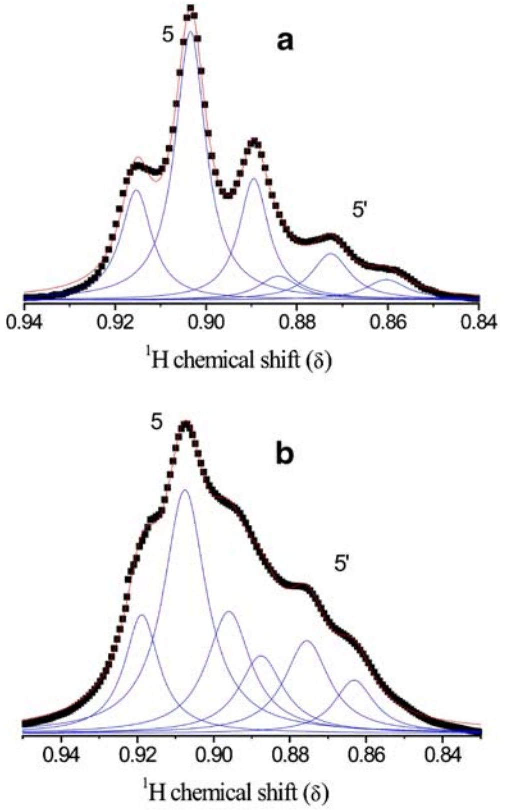

**Fig. 4** Line-shape analysis of the methyl protons at the end of the side alkyl chain of 16-4-16 (**a**) and 16-3-16 (**b**) simulated by Origin 7

**Table 4** Area and $T_1$ and $T_2$ values of the component peaks obtained by deconvolution of the methyl peaks at the end of the side alkyl chain of 16-4-16 and 16-3-16 in the $^1$H NMR spectra, which are shown in Fig. 1

| | 5 | 5′ |
|---|---|---|
| 16-4-16 | | |
| Area | 3.5 | 1 |
| $T_1$ (ms) | 1,258 | 1,363 |
| $T_2$ (ms) | 376 | 430 |
| 16-3-16 | | |
| Area | 1.86 | 1 |
| $T_1$ (ms) | 1,376 | 1,316 |
| $T_2$ (ms) | 226 | 198 |

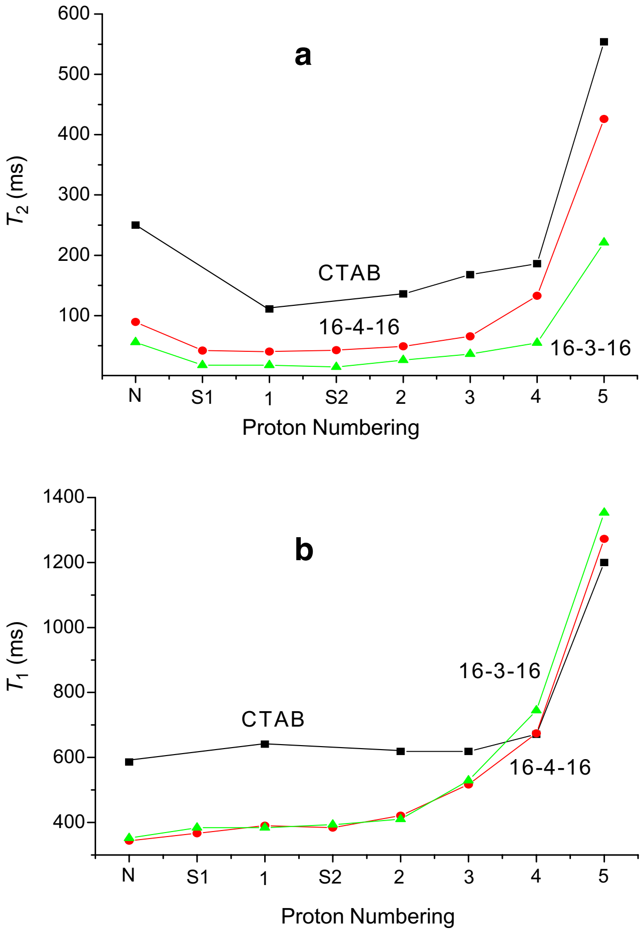

**Fig. 5** $T_2$ (**a**) and $T_1$ (**b**) values of corresponding proton groups of CTAB, 16-4-16, and 16-3-16 solutions at 298, 313, and 318 K, respectively

molecules are involved in the micelle. While the self-diffusion coefficient of the solvent, water, meets the requirements of Einstein–Stokes equation. Its self-diffusion coefficient is proportional to the absolute temperature. The measured value at 318 K seems somewhat higher than expected. This can be attributed to the release of the hydration water molecules bounded to the micelle upon increasing temperature.

### *Effect of the positively charged polar head*

Figure 1 shows $^1$H NMR spectra of CTAB (a), 16-4-16 (b), and 16-3-16 (c). It is noticed that chemical shifts of these protons close to the polar head group show clear dependence on the spacers, with 16-3-16 > 16-4-16 > CTAB, where the shift of the α-methylene protons of the alkyl side chain (1) and the α- and β-methylene protons of the spacer (S1 and S2) is most pronounced. To get some insight into this phenomenon, proton chemical shifts of these surfactants in the single molecular state are needed to distinguish whether this downfield shift originates from the intra-molecular (chemical structure) or from the inter-molecular (micellization) interaction. Unfortunately, obtaining well-resolved 1D spectra of 16-3-16 and 16-4-16 at concentrations below their CMCs was impossible, owing to their low CMCs. So we tried to study their homologues, the 14-*s*-14 series, to shed some light in understanding this downfield effect.

The proton chemical shifts of 14-3-14 and 14-4-14 aqueous solutions, at concentrations which are 0.5 and 10 times their CMCs, are listed in Table 3. It is obvious that chemical shifts of 1, S2, and N protons of 14-3-14 drift downfield farther than those of 14-4-14, respectively, in the single molecular state, showing intra molecular effect. The difference in the chemical shift of S2 protons is most obvious because the distance between the S2 protons and the other ammonium group in the same molecule affects proton chemical shift markedly [31]. The difference shows the effect of the spacer length between the two positively charged ammonium groups in these molecules. Meanwhile, the chemical shift difference for 1 protons is more obvious than that in S1 protons, which are the nearest to the polar head equally. Therefore, 1 protons of 14-3-14 are less shielded and have a larger chemical shift than those of 14-4-14.

Comparison of the proton chemical shift in the molecular state (0.5 CMC) and the micellar state (10 CMC) gives information about intermolecular effect of the positively charged ammonium ions. Table 3 shows the chemical shifts and difference between two states for 14-3-14 and 14-4-14. Upon micellization, resonances of 1, S1, and N are drifted δ

**Table 5** Behavior of the $T_2$ relaxation decay in the 16-3-16 and 16-4-16 solutions at a concentration of ten times their CMCs at 318 and 313 K, respectively

| | 16-4-16 | | | | 16-3-16 | | | |
|---|---|---|---|---|---|---|---|---|
| | $T_2$ (ms) | $T_{2s}$ (ms) | $P_{2s}$ (%) | $T_{2f}$ (ms) | $T_2$ (ms) | $T_{2s}$ (ms) | $P_{2s}$ (%) | $T_{2f}$ (ms) |
| N | 89.6 | 103 | 82.7 | 37.4 | 55.9 | 76.4 | 56.1 | 34.1 |
| 3 | 65.5 | 95.9 | 57.3 | 27.5 | 36.4 | 83.9 | 23.6 | 27.8 |

$T_{2f}$ $T_2$ value of the fast-relaxing component; $T_{2s}$ $T_2$ value of the slow-relaxing part; $P_{2s}$ percentage of the protons exhibiting slow relaxation compared to the total number of protons

0.17, δ 0.17, and δ 0.12, respectively, downfield for 14-3-14, and the corresponding values are, respectively, δ 0.1, δ 0.09, and δ 0.09 for 14-4-14, while the chemical shift changes for the other protons are less than 0.06. These suggest that formation of the micelle has larger effect on the protons close to the polar group than on those of the alkyl side chain away from the polar group. In addition, such effects are weaker in the 14-4-14 system than in the 14-3-14 system. Consequently, the surfactant molecules are less tightly packed in the 14-4-14 micelles than in the 14-3-14 micelles. Considering the fact that S1(1) and N protons of 16-3-16 have larger chemical shifts than those of 16-4-16 (Fig. 1), we may conclude that the 16-3-16 molecules would be more tightly packed in their micelles than the 16-4-16 molecules would be.

### *The compact surface layer and the interior of the micellar core*

*The compact surface layer of the micellar core* The $T_2$ values measured show a similar distribution across entire molecule for the three surfactants, CTAB, 16-4-16, and 16-3-16 (Fig. 5b). It is interesting to note that at all positions, the proton relaxing efficiency is in the same order of CTAB < 16-4-16 < 16-3-16. Since $T_2$ is closely related to local movement, faster relaxing or shorter $T_2$ indicates that the 16-3-16 molecules are much tightly packed in the micelle than that of 16-4-16 and CTAB, respectively. The spacer strengthens the micellar structure, and a three-methylene chain has larger effect than a four-methylene chain. These results are in agreement with the chemical shift measurement. It should be emphasized that the thermodynamic equilibrium distance between the polar heads reported value for CTAB in the micelles is of approximately 0.7–0.9 nm (the distance of between two carbon atoms of the alkyl chain is about 0.1265 nm) [1]. So the distance between the polar heads of CTAB is equal to the length of a spacer chain having six methylene groups. The spacer chain reduces the distance between the polar head groups in the micelle, and this helps to the increase in the density of the polar heads on the micellar surface. The shorter the spacer, the more tightly the hydrophobic chains are packed, and the stronger is the effect in the restriction to the motion of protons.

Distributions of the $T_1$ values across the surfactants are similar to those of the $T_2$ values, with the exception of *N*-methyl becoming the fastest one, and the differences between 16-3-16 and 16-4-16 become less significant (Fig. 5b). This is due to different relaxation mechanism of $T_1$ and $T_2$. The larger $T_1$ values, or slower relaxation, of the alkyl side chain protons (3, 4, and 5) indicate that these parts of the surfactants are in a hydrophobic environment of the micelles. While the protons (N, 1, 2, S1, and S2) with short $T_1$ values, or fast relaxation, are situated in the palisade layer.

In our previous study, simulation of the decay curves of proton relaxation for micellar solutions showed that the relaxation decay curves of $T_2$ of some of the protons on the hydrophobic chains are bi-exponential. The fast-relaxing component is attributed to the protons situated near or on the surface of the micellar core, the palisade layer, while the slower one is attributed to the remaining protons in the interior [32]. From Table 5, one can note that the simulation of the relaxation decay of N and 3 protons manifests bi-exponential behavior, and the $T_{2f}$ and $T_{2s}$ values of 16-3-16 protons are in the order of those of 16-4-16, respectively. However, there is a significant difference in the fraction of the fast and slow components in these two systems. The fast relaxation components of N and 3 of 16-3-16 are larger than those of 16-4-16, respectively, which implies that larger fractions of N and 3 protons of 16-3-16 participate in the formation of the palisade layer in 16-3-16 micelles than those of the corresponding protons in 16-4-16 micelles. This also suggests that a longer segment of the 16-3-16 side alkyl chain stays in the micelle palisade layer formation than that of 16-4-16.

*The interior of the micellar core* Carefully examining Fig. 1 one finds that the end methyl proton resonances of 16-3-16 and 16-4-16 are overlapped peaks, while that of CTAB is not. The line-shape of an overlapped peak can be deconvolved into a number of peaks [33]. So, the overlapped methyl proton resonances of 16-3-16 and 16-4-16 solutions were deconvolved into two triplets, characteristic of two methyl protons as shown in Fig. 4a and b, namely 5 and 5′, respectively. This suggests that the methyl protons at the end of the side alkyl chains of 16-3-16 and 16-4-16

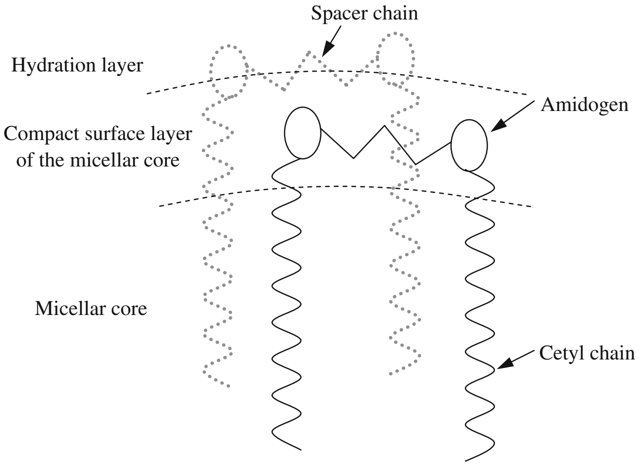

**Fig. 6** The section sketch map for the arrangement of the gemini surfactant 16-3-16 molecules in its micelles, the dashed molecule is situated on the *top* of the full molecule

reside in two different chemical environments, respectively. Relaxation characteristics of the deconvolved two triplets (5 and 5′) of 16-3-16 differ not much, the same as those of 16-4-16, shown in Table 4. This shows that the two end-methyl groups of the 16-3-16 micelles are situated in different environments of the micellar core interior and so as for the two methyl groups of 16-4-16 micelles. The two deconvolved proton peaks do not seem to stand for the monomeric and the micellar states because the concentrations of the surfactants are ten times their CMCs, i.e., the ratio between the areas of the two triplets should be 1:9 in each solution. However, it is obvious from Table 5 that the area ratios of 5:5′ of 16-3-16 and 16-4-16 differ markedly from 1:9, respectively. All of these suggest that the two environments are in the interior of the hydrophobic micellar core region. These two environments may be attributed to the special arrangement of the surfactant molecules in the micellar core, i.e., a part of molecules sitting on the other molecules at a certain angle to favor the reduction of inter-distances between the polar heads in the micelle. Surfactant molecules involved in the micelle are relatively fixed for its big polar head group and the rigid spacer chain, so these two states would not exchange very fast. Consequently, the environments of methyl groups of the surfactant molecules sitting on and being underneath will be different. The sketch map is shown in Fig. 6. Similar effect can exist for other protons nearer to the polar head region. However, the less distant from the polar head region, the smaller is the effect. So, double peaks for 1–3 and N protons are not observed. As for 4 proton resonance peak, a sum of seriously overlapped proton resonance of 12 methylene groups, although being nearest to the end methylene protons, this effect will not be resolved. This is accordant with the former conclusion, i.e., the head groups are in a saw-toothed form staying at the surface of the micelle as shown in Fig. 6.

## Summary

In conclusion, the combination of the chemical shift changes, line-shape analysis of the $^1$H NMR methyl proton signals, self-diffusion coefficient and relaxation measurements, and the inter-proton distances deduced from the 2D NOESY experiment show that these spherical micelles are formed in 16-3-16 solution at a concentration of 0.26 mmol/l at 318 K. The 16-3-16 micelles exhibit unique properties due to the shorter length of spacer chain. Its side alkyl chains are packed more tightly, the spacer chain is more rigid, and the density of *N*-methyl groups on the micellar surface of 16-3-16 micelle is larger than that of 16-4-16.

**Acknowledgments** The financial support by the National Natural Science Foundation of China (20610104 and 20635040) is gratefully acknowledged.

## References

1. Zana R (2002) Adv Colloid Interface Sci 97:205–253
2. Menger FM, Keiper JS (2000) Angew Chem Int Ed 39:1906–1920
3. Zana R, Benrraou M, Rueff R (1991) Langmuir 7:1072–1075
4. Menger FM, Littau CA (1993) J Am Chem Soc 115:10083–10090
5. Zana R (2002) J Colloid Interface Sci 252:259–261
6. Wettig SD, Verrall RE (2001) J Colloid Interface Sci 235:310–316
7. Oliviero C, Coppola L, Mesa CL, Ranieri GA, Terenzi M (2002) Colloids Surf A 201:247–260
8. Aswal VK, Goyal PS, De S, Bhattacharya S, Amenitsch H, Bernstorff S (2000) Chem Phys Lett 329:336–340
9. Han LJ, Chen H, Luo PY (2004) Surf Sci 564:141–148
10. Goyal PS, Aswal VK (2001) Curr Sci 80(8):972–979
11. Alami E, Beinert G, Marie P, Zana R (1993) Langmuir 9:1465–1467
12. Danino D, Talmon Y, Zana R (1995) Langmuir 11(5):1448–1456
13. Aswal VK, De S, Goyal PS, Bhattacharya S, Heenan RK (1998) J Chem Soc Faraday Trans 94:2965–2967
14. Wettig SD, Verrall RE, Li XF (2003) Langmuir 19:3666–3670
15. Grosmaire L, Chorro M, Chorro C, Partyka S, Zana R (2002) J Colloid Interface Sci 246:175–181
16. Rosen MJ, Song LD (1996) J Colloid Interface Sci 179:261–268
17. Grosmaire L, Chorro M, Chorro C, Partyka S, Lagerge S (2001) Thermochim Acta 379:255–260
18. Borse M, Sharma V, Aswal VK, Goyal PS, Devi S (2005) J Colloid Interface Sci 284:282–288
19. Laschewsky A, Lunkenheimer K, Rakotoaly RH, Wattebled L (2005) Colloid Polym Sci 283:469–479
20. Hirata H, Hattori N, Ishida M, Okabayashi H, Frusaka M, Zana R (1995) J Phys Chem 99:17778–17784
21. Zana R, Talmon Y (1993) Nature 362:228–230
22. Zana R (2002) J Colloid Interface Sci 246:182–190
23. Missel PJ, Mazer NA, Benedek GB, Young CY, Carey MC (1980) J Phys Chem 84:1044–1057
24. Du YR, Zhao S, Shen LF (2002) Annu Rep NMR Spectrosc 48:246–295
25. Liu AH, Chen H, Cheng GZ, Fang XW, Yang XY, Mao SZ, Yuan HZ, Luo PY, Du YR (2005) Chin J Magn Reson 22(2):123–131
26. Cui XH, Chen H, Yang XY, Liu AH, Mao SZ, Cheng GZ, Yuan HZ, Luo YP, Du YR (2007) Acta Phys Chim Sin 23(3):317–321
27. Fendler JH (1982) Membrane mimetic chemistry. Wiley, New York
28. Jerschow A, Muller N (1997) J Magn Reson 125:372–375
29. Stejskal EO, Tenner JE (1965) J Chem Phys 42:288–293
30. Ernst RR, Bodenhausen G, Wokaun A (1987) A principles of nuclear magnetic resonance in one and two dimensions. Oxford University Press, New York
31. Luo MD, Yan XC, Zhang GY (2002) China Surfactant Deterg Cosmet 32(3):5–7
32. Zhao S, Yuan HZ, Yu JY, Du YR (1998) Colloid Polym Sci 276:1125–1130
33. Liu ML, Tang HR, Nicholson JK, Lindon JC (2002) Magn Reson Chem 40:S83–S88